Polyakov loop models in the large N limit: Correlation function and screening masses

O. Borisenko,[1,2,*] V. Chelnokov,[3,†] and S. Voloshyn[2,‡]

[1]*INFN Gruppo Collegato di Cosenza, Arcavacata di Rende, 87036 Cosenza, Italy*
[2]*Bogolyubov Institute for Theoretical Physics, National Academy of Sciences of Ukraine, 03143 Kyiv, Ukraine*
[3]*Institut für Theoretische Physik, Goethe-Universität Frankfurt, 60438 Frankfurt am Main, Germany*

(Received 10 November 2023; accepted 8 April 2024; published 9 May 2024)

We explore the 't Hooft-Veneziano limit of the Polyakov loop models at finite baryon chemical potential. Using methods developed by us earlier we calculate the two- and N-point correlation functions of the Polyakov loops. This gives a possibility to compute the various potentials in the confinement phase and to derive the screening masses outside the confinement region. In particular, we establish the existence of complex masses and an oscillating decay of correlations in a certain range of parameters. Furthermore, it is shown that the calculation of the N-point correlation function in the confinement phase reduces to the geometric median problem. This leads to a large N analog of the Y law for the baryon potential.

DOI: 10.1103/PhysRevD.109.094503

I. INTRODUCTION

The characteristics of strongly interacting matter at high temperatures and densities are actively studied through theoretical and computational methods. The phase diagram of quantum chromodynamics (QCD), which shows how strongly interacting matter behaves as temperature and baryon density change, is currently a subject of intense investigation. Studying the QCD phase diagram is crucial in gaining insights into the fundamental properties of matter under extreme conditions, such as those one encounters in heavy ion collisions or within compact astrophysical objects.

It is well known that the introduction of a chemical potential μ into the QCD action makes the Euclidean path integral measure complex, so standard Monte Carlo simulations are not feasible. Over the last few decades, various approaches have been developed to tackle this sign problem either partially or entirely. Some notable methods include Taylor expansion or reweighting at low chemical potential, simulations at imaginary potential, complex Langevin simulations, and others as reviewed in [1,2]. Despite certain progress achieved within these methods, lattice simulations at arbitrary real chemical potential are not yet possible.

Analytical efforts to overcome the sign problem are mainly concentrated around some effective theories, like the Polyakov loop models, with the goal to map such theories via the duality transformations to models with the positive Boltzmann weight, see [3–7]. Another direction of analytical attempts is investigation of the 't Hooft and the 't Hooft-Veneziano limits of lattice QCD. For example, using methods developed in [8,9], the large N limit was explored for $U(N)$ Polyakov loop models in [10,11]. Extension of these methods to $SU(N)$ models was accomplished in Refs. [12–14]. In these papers we established a general phase structure of the model in the 't Hooft-Veneziano limit. An important open problem is the behavior of the Polyakov loop correlations in this limit. This problem is addressed in the present paper. The large distance decay of the Polyakov loop correlations at finite chemical potential is governed by the (electric and magnetic) screening masses. For a general review on screening masses, we refer the reader to [15]. In Refs. [16,17] these masses have been computed in lattice QCD with imaginary chemical potential. Relatively little is known about screening masses in the presence of the real chemical potential. Some results obtained from the simulations of the dual of the $SU(3)$ Polyakov loop model can be found in Refs. [18,19].

A closely related problem is the emergence of the complex spectrum at finite density. This leads to an exponential decay of the correlations modulated by an oscillating function [20–23]. Locating such a liquid phase requires the computation of long-distance correlations with real chemical potential. So far, a phase with an oscillating decay of correlations was shown to exist in $(1+1)d$ lattice gauge theory (LGT) with heavy quarks in [21] and in $Z(3)$ spin model in a complex external field in [22]. The latter

*oleg@bitp.kyiv.ua
†chelnokov@itp.uni-frankfurt.de
‡s.voloshyn@bitp.kyiv.ua

result was extended to many $Z(N>3)$ models in [23]. Here we prove that the liquid phase exists in the 't Hooft-Veneziano limit of the Polyakov loop model in a certain range of parameters. Preliminary results of this study have been presented in [13].

We work with the Polyakov loop model whose action is given by

$$S=\beta\sum_{x,n}\mathrm{Re}W(x)W^*(x+e_n)+\sum_x\sum_{f=1}^{N_f}h(m_f)\left(e^{\mu}W(x)+e^{-\mu}W^*(x)\right). \quad (1)$$

Here, $W(x)=\mathrm{Tr}U(x), U(x)\in U(N), SU(N)$, $\beta=\beta(g^2,N_t)$ is an effective coupling constant, $h(m_f)$ is a function of the quark mass m_f, and N_f is a number of fermion flavors. Our goal is to calculate the correlation functions of this model in the 't Hooft-Veneziano limit [24,25]: $g\to 0$, $N\to\infty$, $N_f\to\infty$ such that the product g^2N and the ratio $N_f/N=\kappa$ are kept fixed. For the case of N_f degenerate flavors considered here, one has $\sum_{f=1}^{N_f}h(m_f)=N_fh(m)\to N\kappa h(m)\equiv N\alpha$. In the previous papers [13,14] we derived the large-N representation for the partition function of the model (1) and described its phase diagram. In particular, a third order phase transition separating two phases has been found.

Let us briefly describe the large N representation which is the starting point of the following calculations. Consider the following change of variables in the partition function $\rho(x)\cos\omega(x)=1/N\mathrm{Re}W(x)$, $\rho(x)\sin\omega(x)=1/N\mathrm{Im}W(x)$. If $\eta(x)$ ($\bar\eta(x)$) is the power of the Polyakov loop (its conjugate) then the arbitrary correlation function can be written down as [14]

$$\Gamma=e^{\mu\sum_x(\bar\eta(x)-\eta(x))}\left\langle\prod_x\rho(x)^{\eta(x)+\bar\eta(x)}e^{i\omega(x)(\eta(x)-\bar\eta(x))}\right\rangle. \quad (2)$$

The expectation value in the last expression refers to the following partition function:

$$Z=\prod_x\int_0^1\rho(x)d\rho(x)\int_0^{2\pi}\frac{d\omega(x)}{2\pi}\times\int_{-\infty}^{\infty}du(x)dt(x)ds(x)\,e^{N^2S_{\mathrm{eff}}}. \quad (3)$$

Making the shift $\omega\to\omega+i\mu$, one obtains for the effective action

$$\begin{aligned}S_{\mathrm{eff}}&=\beta\sum_{x,n}\rho(x)\rho(x+e_n)\cos(\omega(x)-\omega(x+e_n))+\alpha\sum_x\rho(x)\cos\omega(x)\\&\quad+\mu\sum_x u(x)+\sum_x V(\rho(x),\omega(x);u(x),t(x),s(x)),\\V(\rho,\omega;u,t,s)&=-iu\omega+\frac{3}{2}|u|-\frac{1}{2}(1+|u|)^2\ln(1+|u|)+\frac{1}{2}u^2\ln|u|-2i\rho s\\&\quad+|u|\ln(t+is)-t^2-s^2-\sum_{k=0}^{\infty}(t^2+s^2)^{k+1}C_k(|u|).\end{aligned} \quad (4)$$

The function $C_k(|u|)$ is given in the Appendix. This representation was derived in our previous paper [14] with a general type of the gauge action. The phase diagram of the model (3) with the action (4) was thoroughly studied in [14]. It was found the model exhibits the phase transition of third order on the surface $z=0$, where z is defined as

$$z=\mu-\ln\left(1+\sqrt{1-\frac{\alpha^2}{(1-\beta d)^2}}\right)+\ln\frac{\alpha}{1-\beta d}+\sqrt{1-\frac{\alpha^2}{(1-\beta d)^2}}. \quad (5)$$

In the region $z>0$ the $SU(N)$ partition function gets a nontrivial dependence on the chemical potential. This can be explained as follows. Because $SU(N)$ reduces to $U(N)$ in the large-N limit, naively one would expect the same happens for the partition functions of both theories. Indeed, this is the case when the charge conjugation symmetry is not broken and static quarks and antiquarks have the same weights in the fermion determinant. When nonzero baryon chemical potential is added, the charge conjugation symmetry is broken, weights are different, and this results in different answers for the partition functions with $U(N)$ and $SU(N)$ groups. $U(N)$ partition function does not depend on μ (this is a consequence of the absence of baryon states in this model) whereas $SU(N)$ partition

function depends on μ in a certain region of parameters (quark masses and coupling constant). We proved this explicitly in our paper [12].

In this paper we derive the large-N representation for the arbitrary correlation function (2) and study two- and N-point functions in details. It turns out that in the 't Hooft-Veneziano limit the correlation function reduces to a product of the Polyakov loop expectation values. Therefore, in order to get a nontrivial dependence of the correlations on the distances between static quarks one has to evaluate the first nontrivial correction to the 't Hooft-Veneziano limit. This can be done by an expansion around the saddle-point large-N solution and performing an integration over fluctuations.

The rest of the paper is organized as follows. In Sec. II we calculate the general form of the correlation function and study the behavior of the screening masses. Complex masses appearing above the phase transition are described in details. In Sec. III the N-point function related to baryon potential is evaluated in the confinement phase of the pure gauge theory. Section IV presents our summary.

II. CORRELATION FUNCTIONS AND SCREENING MASSES

In this section we calculate various correlation functions and corresponding screening masses in the large N limit. As is well known, at nonzero chemical potential the Polyakov loop correlations form a correlation matrix [17]

$$\Gamma(x,y)=\begin{pmatrix}\left\langle \frac{1}{N}\mathrm{Re}W(x)\frac{1}{N}\mathrm{Re}W(y)\right\rangle_c & \left\langle \frac{1}{N}\mathrm{Re}W(x)\frac{1}{N}\mathrm{Im}W(y)\right\rangle_c\\ \left\langle \frac{1}{N}\mathrm{Im}W(x)\frac{1}{N}\mathrm{Re}W(y)\right\rangle_c & \left\langle \frac{1}{N}\mathrm{Im}W(x)\frac{1}{N}\mathrm{Im}W(y)\right\rangle_c\end{pmatrix}=\begin{pmatrix}\Gamma_{rr} & \Gamma_{ri}\\ \Gamma_{ri} & \Gamma_{ii}\end{pmatrix}, \tag{6}$$

where $\langle\ldots\rangle_c$ refers to a connected part of the correlation. To give the definition for Γ_{rr}, Γ_{ri}, and Γ_{ii} in terms of (2), we introduce the following correlations:

$$\begin{aligned}
\Gamma_{qq}&\equiv\Gamma(\eta(x)=1,\eta(y)=1)=\left\langle\frac{1}{N}W(x)\frac{1}{N}W(y)\right\rangle,\\
\Gamma_{q\bar{q}}&\equiv\Gamma(\eta(x)=1,\bar{\eta}(y)=1)=\left\langle\frac{1}{N}W(x)\frac{1}{N}W^*(y)\right\rangle\\
&=\Gamma(\bar{\eta}(x)=1,\eta(y)=1)=\left\langle\frac{1}{N}W^*(x)\frac{1}{N}W(y)\right\rangle,\\
\Gamma_{\bar{q}\bar{q}}&\equiv\Gamma(\bar{\eta}(x)=1,\bar{\eta}(y)=1)=\left\langle\frac{1}{N}W^*(x)\frac{1}{N}W^*(y)\right\rangle,\\
M&\equiv\Gamma(\eta(0)=1)=\left\langle\frac{1}{N}W(0)\right\rangle,\qquad M^*\equiv\Gamma(\bar{\eta}(0)=1)=\left\langle\frac{1}{N}W^*(0)\right\rangle.
\end{aligned} \tag{7}$$

In (7) all sources $\eta,\bar{\eta}$ apart from those explicitly mentioned are assumed to be zero. Then, we can write

$$\begin{aligned}
\Gamma_{rr}&=\frac{1}{4}(\Gamma_{qq}+2\Gamma_{q\bar{q}}+\Gamma_{\bar{q}\bar{q}}-(M+M^*)^2),\\
\Gamma_{ii}&=-\frac{1}{4}(\Gamma_{qq}-2\Gamma_{q\bar{q}}+\Gamma_{\bar{q}\bar{q}}-(M-M^*)^2),\\
\Gamma_{ri}&=\frac{1}{4i}(\Gamma_{qq}-\Gamma_{\bar{q}\bar{q}}-M^2+M^{*,2}).
\end{aligned} \tag{8}$$

When $\mu=0$ the off-diagonal terms Γ_{ri} vanish and the coefficients in the exponential decay of diagonal terms define the magnetic and electric screening masses

$$\Gamma_{rr}\simeq\frac{e^{-m_M R}}{R^\eta},\qquad \Gamma_{ii}\simeq\frac{e^{-m_E R}}{R^\eta},\qquad R=|x-y|. \tag{9}$$

When $\mu>0$ the electric and magnetic sectors mix, so each correlation matrix element is a sum of two terms—one decaying with m_M and the other with m_E.

In the limit $N\to\infty$ the model exhibits so-called "large N factorization" [24]. This means all correlations become trivial in the sense they are reduced to the product of averages of Polyakov loops. For example, the expectation value of the Polyakov loop equals $\rho_0 e^{\pm i\omega_0}$ and the invariant two-point correlation function is simply ρ_0^2. Therefore, to get a nontrivial dependence of correlation functions on the

distances we need to take into account the fluctuations around the large-N solution. In the limit $N \to \infty$ all integrals in (3) are evaluated by the saddle-point method (see, [14] for details). In what follows we denote by ρ_0, ω_0, u_0, t_0, s_0 the corresponding saddle points. For the $SU(N)$ model the full analytic solution can be obtained near the critical surface $z = 0$. For completeness, we give this solution in the Appendix. Performing the shift $\rho(x) \to \rho_0 + \frac{1}{N}\rho(x)$ and similar ones for other saddles, we expand the full action around saddle points. The leading contribution to the correlation function arises from the Gaussian fluctuations. The Gaussian integrals over u, t, s variables are factorized as can be seen from the form of the effective action (4). Evaluating these Gaussian integrals leads to the following representation for the correlation function:

$$\Gamma = \prod_x \rho_0^{\eta(x)+\bar{\eta}(x)} e^{(i\omega_0-\mu)(\eta(x)-\bar{\eta}(x))} \frac{1}{Z}\int_{-\infty}^{\infty}\prod_x d\rho(x)d\omega(x)\, e^{\sum_x[-\frac{1}{\rho_0 N}(\eta(x)+\bar{\eta}(x))\rho(x)-\frac{i}{N}(\eta(x)-\bar{\eta}(x))\omega(x)]+S_{\text{fluct}}}, \tag{10}$$

$$S_{\text{fluct}} = \sum_{x,n}\left[\beta\rho(x)\rho(x+e_n) - \frac{1}{2}\beta\rho_0^2(\omega(x)-\omega(x+e_n))^2\right] + \sum_x [a_1\rho^2(x) - a_3\omega^2(x) + ia_2\rho(x)\omega(x)], \tag{11}$$

where the coefficients a_i are functions of saddle points (their explicit form is not important here). Two remaining Gaussian integrals are less trivial but quite the standard ones. The final result of the integration is presented in Eqs. (13)–(15) below. In those equations we use the following lattice Green's function:

$$G_{x,x'}(m) = \frac{1}{L^d}\sum_{k_n=0}^{L-1}\frac{e^{\frac{2\pi i}{L}\sum_n^d k_n(x_n-x'_n)}}{m+f(k)}, \qquad f(k) = d - \sum_{n=1}^{d}\cos\frac{2\pi}{L}k_n. \tag{12}$$

A. Correlation functions in $SU(N)$ model

Evaluating the Gaussian integrals in the second line of (10) we arrive at the following general result when $z > 0$:

$$\Gamma = \prod_x e^{(\mu-i\omega_0)(\bar{\eta}(x)-\eta(x))}\rho_0^{(\eta(x)+\bar{\eta}(x))}\exp\left[\frac{1}{4N^2\beta\rho_0^2}\sum_{x,x'}(A_1(x,x')+A_2(x,x'))\right] \tag{13}$$

$$A_1(x,x') = \frac{1}{\sqrt{C_1C_2}}(C_1\eta(x)\eta(x') + C_2\bar{\eta}(x)\bar{\eta}(x'))(G_{x,x'}(m_-) - G_{x,x'}(m_+)), \tag{14}$$

$$A_2(x,x') = 2\eta(x)\bar{\eta}(x')(G_{x,x'}(m_-) + G_{x,x'}(m_+)). \tag{15}$$

The masses m_+ and m_- are given by

$$m_\pm = \frac{1}{2\beta\rho_0^2}\left(C_3 \pm \sqrt{C_1C_2}\right), \tag{16}$$

where the constants C_i are defined as

$$C_{1,2} = b_2 + (d\beta - b_1)\rho_0^2 \pm ib_3\rho_0,$$
$$C_3 = b_2 - (d\beta - b_1)\rho_0^2. \tag{17}$$

This result means that in the general case the masses $m_\pm$ can be complex. Coefficients b_i are given in the Appendix, Eqs. (A1)–(A3). This result allows one to compute any observable above the critical surface $z > 0$ by choosing the appropriate values of the sources $\eta(x)$ and $\bar{\eta}(x)$. The expectation value of the Polyakov loop $M = \langle\rho(x)e^{i\omega(x)}\rangle$ becomes

$$M = \rho_0 e^{i\omega_0}\exp\left[\frac{C_1}{4N^2\beta\rho_0^2\sqrt{C_1C_2}}(G_0(m_-) - G_0(m_+))\right], \tag{18}$$

where $G_0(m)$ is the zero distance Green's function. When masses are real and $m_- \le m_+$ one obtains for the eigenvalues of the correlation matrix (6) in the limit of a large separation R

$$\mathcal{M}_1 = \frac{MM^*}{2N^2\beta\rho_0^2} G_R(m_-), \tag{19}$$

$$\mathcal{M}_2 = \begin{cases} \frac{MM^*}{2N^2\beta\rho_0^2} G_R(m_+), & \text{if } m_- \le m_+ \le 2m_-, \\ \frac{MM^*}{2N^2\beta\rho_0^2}\left(G_R(m_+) + \frac{1}{16N^2\beta\rho_0^2}\left(2 - \frac{C_1+C_2}{\sqrt{C_1C_2}}\right)G_R^2(m_-)\right), & \text{if } m_+ \ge 2m_-. \end{cases} \tag{20}$$

When masses are complex, $m_- = m_+^*$, the Green's functions $G_R(m_\pm)$ also become complex, $G_R(m_-) = G_R(m_+)^*$. The correlation matrix eigenvalues can be described by (19) and the top line of (20). These formulas generalize the notion of the magnetic and the electric masses: $m_\pm$ could be considered as $\mu \neq 0$ analog of the magnetic and electric masses m_M, m_E.

The leading linear terms in $G_R(m_\pm)$ of the elements of the correlation matrix are found to be

$$\Gamma_{rr} = D\left[(\sqrt{C_1}M + \sqrt{C_2}M^*)^2 G_R(m_-) - (\sqrt{C_1}M - \sqrt{C_2}M^*)^2 G_R(m_+)\right], \tag{21}$$

$$\Gamma_{ii} = D\left[(\sqrt{C_1}M + \sqrt{C_2}M^*)^2 G_R(m_+) - (\sqrt{C_1}M - \sqrt{C_2}M^*)^2 G_R(m_-)\right], \tag{22}$$

$$\Gamma_{ri} = -iD[(C_1M^2 - C_2M^{*,2})(G_R(m_-) - G_R(m_+))], \qquad D = \frac{1}{8N^2\beta\rho_0^2\sqrt{C_1C_2}}. \tag{23}$$

B. Phase diagram and complex masses

The general phase structure of the $SU(N)$ model has been described in [14]. Figure 1 shows cross sections of the phase diagram for a fixed value of βd (left panel) and a fixed value of α (left panel), $d = 3$. These cross sections reveal three regions of the phase diagram which can be characterized by a different behavior of correlation functions and screening masses.

Region I. Here, one finds a single mass equal to the mass in the $U(N)$ model for the same values of parameters. The free energy and correlation functions do not depend on the chemical potential. Crossing the transition line (blue line in Fig. 1 along which $C_1 = C_2 = 0$) one enters the region III which becomes more and more narrow with μ increasing. Analytical expressions for the masses can be found in the vicinity of this transition line using explicit formulas for

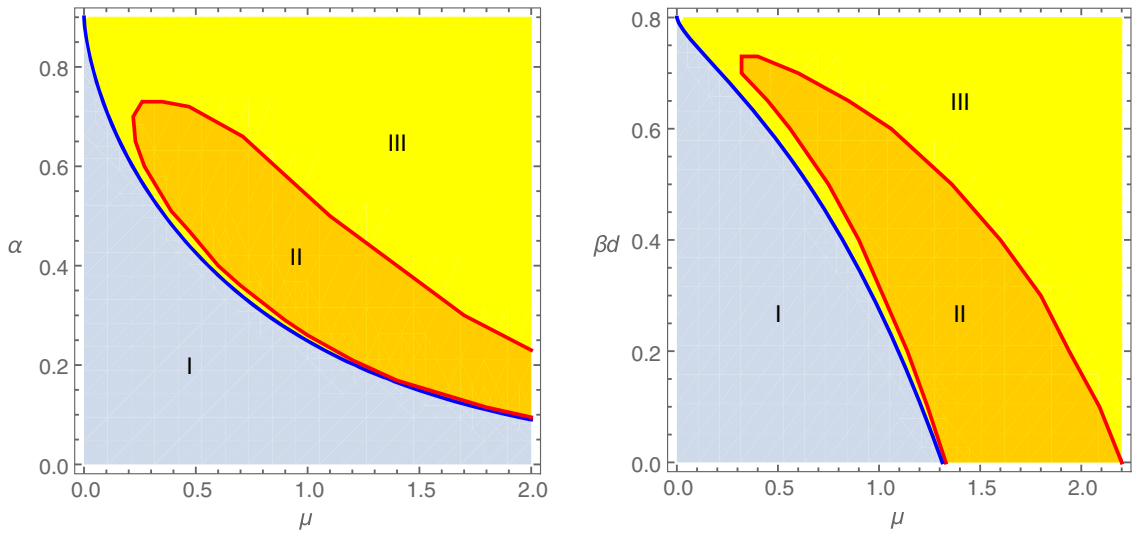

FIG. 1. Cross sections of the phase diagram of the SU(N) model. Left: μ–α coordinates at fixed $\beta d = 0.1$. Right: μ–βd coordinates at fixed $\alpha = 0.2$. The blue curve shows the critical line of the third order phase transition. See text for details.

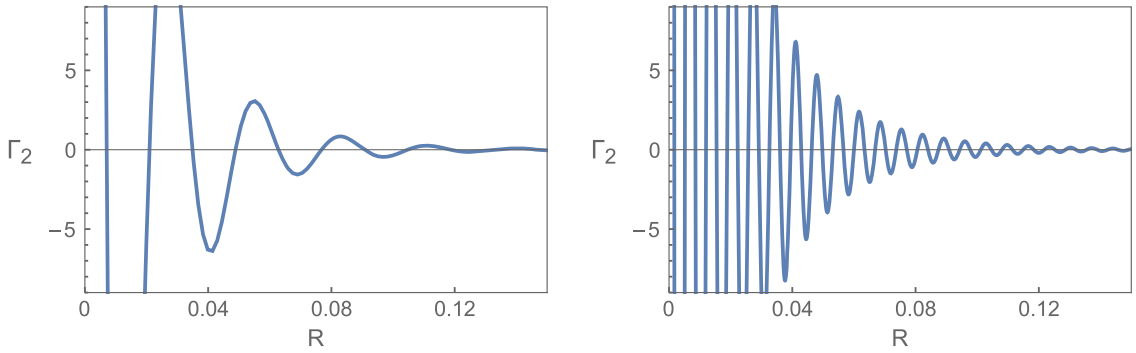

FIG. 2. Oscillating decay of the correlation function with a distance in region II of the phase diagram. Left: $m_i/m_r \approx 7$, $\alpha = 0.05$, $\beta d = 0.1$, $\mu = 2.595$. Right: $m_i/m_r \approx 30$, $\alpha = 0.01$, $\beta d = 0.1$, $\mu = 4.1935$.

coefficients b_i and saddle points given in the Appendix. One finds

$$m_\pm = \frac{1}{\beta} - d - \frac{2}{\beta(4+\ln\frac{z^2}{1-\frac{\alpha^2}{(\beta d-1)^2}})} \mp \frac{2}{\beta(4+\ln\frac{z^2}{1-\frac{\alpha^2}{(\beta d-1)^2}})} + \mathcal{O}(z). \tag{24}$$

Region II. Crossing the lower red line in Fig. 1 the system moves to a phase, where a complex spectrum emerges. Masses m_+ and m_- become conjugate to each other: $m_+ = m_-^* = m_r + i m_i$. The connected part of the two-point correlation is

$$\Gamma_2(R) \approx MM^*(G_R(m_+) + G_R(m_-)) \sim \frac{e^{-m_r R}}{R}\cos m_i R, \tag{25}$$

i.e. it has an exponential decay modulated by the cosine function.

For sufficiently small α and βd, the region $m_i > m_r$ is bounded from above by $\rho \approx 0.41$. In this region the boundary has very small dependence on other parameters. A maximum of the ratio m_i/m_r is reached close to the phase transition and becomes larger when α and βd decrease. As a result, the smaller α and β are, the more profound oscillations are observed. The corresponding behavior of the two-point correlation function is reflected in Fig. 2.

Region III. Separated from region II by a red line on Fig. 1, region III has two distinct real masses and correlations decay exponentially according to Eqs. (21)–(23). The equation defining the red line reads $C_2 = 0$. This line does not define a genuine phase transition, since the

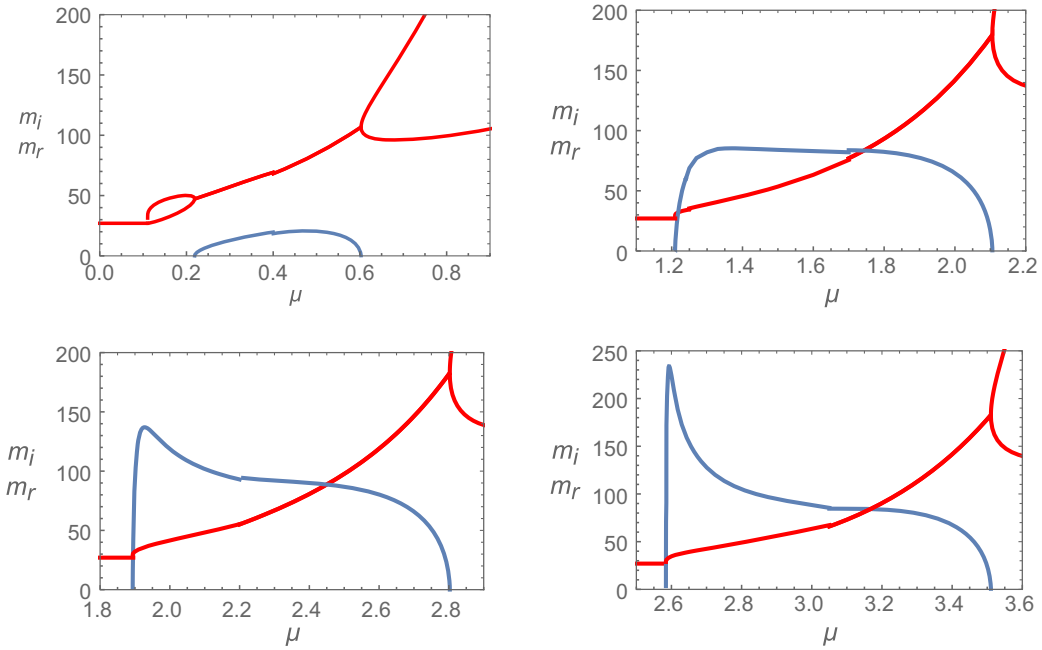

FIG. 3. Real (red) and imaginary (blue) parts of the screening masses vs μ at fixed $\beta d = 0.1$ and fixed $\alpha = 0.7$ (top left), $\alpha = 0.2$ (top right), $\alpha = 0.1$ (bottom left), $\alpha = 0.05$ (bottom right). See text for details.

partition function together with all its derivatives remains analytical in the thermodynamic limit.

Finally, Fig. 3 shows the screening masses as a function of μ for $\beta d = 0.1$ and several values of α. Two real masses above the third order phase transition can be only seen on the top left panel (red line). When α is decreasing, region III gets narrower and two masses become hardly distinguishable. Values of μ, where the imaginary part is not zero, define region II of the phase diagram. A maximum of the imaginary part is located close to the smallest μ value. In the upper region III the imaginary part of the mass vanishes and the real mass splits into two. The larger one has a sharp increase, while the smaller one starts increasing when μ is large enough.

The most important and interesting result of this study is the demonstration that in a certain region of parameters—coupling constant, quark mass, and chemical potential—the spectrum of the theory is complex. The average value of the Polyakov loop is not sensitive to complex masses, as is seen from Eq. (18). Indeed, it is always real on the saddle-point solutions. To reveal the mass spectrum of the theory one has to study the long-distance correlation functions. In the present case it is sufficient to study the correlation functions of the Polyakov loops. In the region where masses are complex, these correlations exhibit exponential decay modulated by a cosine function. Similar oscillating (also called liquid) phase was found earlier in other models. This phase was shown to exist in $(1+1)$-dimensional SU(3) LGT at finite chemical potential [21]. Here, the model was studied in the static approximation for the quark determinant and the spectrum was calculated using the transfer matrix method. Reference. [22] explored $Z(3)$ Potts model in an external complex field in one (via the transfer matrix) and three dimensions (via the mean-field and MC simulations of the dual theory). Here, the correlations of $Z(3)$ spins exhibit the oscillating behavior in a certain range of parameters. Finally, the oscillating phase exists in all $(1+1)$-dimensional $Z(N)$ lattice gauge theories in a static approximation for the quark determinant [23]. The common feature of all of these models is the presence of the chemical potential which makes the effective action complex. It is thus impossible to simulate these actions via the conventional Monte Carlo algorithms due to a severe sign problem. It is necessary to use either analytical methods to study such systems or to map the original theory with a complex action to a dual theory with a positive Boltzmann weight. Both approaches cannot be applied to a full QCD with dynamical fermions; therefore, one should restrict to approximations like the one used here. We think it is instructive to see the emergence of the oscillating phase in the 't Hooft-Veneziano limit. The question whether this phase can be realized in the $SU(3)$ QCD remains open.

C. Two-point functions in $U(N)$ model

$U(N)$ models are easier to study due to a much simpler saddle-points structure, $u_0 = t_0 = \omega_0 = 0$. The dependence on the chemical potentials drops out from the invariant correlation functions. To analyze the correlations in the $U(N)$ model one uses Eqs. (13)–(15) together with the following saddle-point solutions [14]:

$$s_0 = -i\left(\frac{\alpha}{2} + \beta d\rho_0\right),$$
$$\rho_0 = \begin{cases} \frac{\alpha}{2(1-\beta d)}, & \alpha + \beta d \le 1, \\ \frac{1}{4\beta d}\left(2\beta d - \alpha + \sqrt{(2\beta d+\alpha)^2 - 4\beta d}\right), & \alpha + \beta d \ge 1. \end{cases} \tag{26}$$

In the pure gauge case, $\alpha = 0$, one observes a first order confinement-deconfinement phase transition. The expectation value of the Polyakov loop jumps from zero to $1/2$ at the critical point. When α is nonzero, the system undergoes the third order phase transition. Accordingly, we describe two-point correlations for these cases.

(1) $\alpha = 0$, confinement phase:

$$\Gamma_2(R) = \langle W(0)W^*(R)\rangle = \frac{1}{\beta N^2} G_R(m_1),$$
$$m_1 = \frac{1}{\beta} - d. \tag{27}$$

(2) $\alpha = 0$, deconfinement phase:

$$\Gamma_2(R) = \rho_0^2 \exp\left[\frac{1}{2\beta\rho_0^2 N^2}\left(G_0(m_2) + G_R(m_2) - G_0(0) + G_R(0)\right)\right],$$
$$m_2 = \frac{1}{\beta}\left(1 - \sqrt{1 - 1/\beta d}\right)^{-2} - d. \tag{28}$$

(3) $\alpha \neq 0$, confinement phase:

$$\Gamma_2(R) = \rho_0^2 \exp\left[\frac{1}{\beta\rho_0^2 N^2} G_R(m_1)\right]. \tag{29}$$

(4) $\alpha \neq 0$, deconfinement phase:

$$\Gamma_2(R) = \rho_0^2 \exp\left[\frac{1}{2\beta\rho_0^2 N^2}\left(G_0(m_3) + G_R(m_3) - G_0(m_4) + G_R(m_4)\right)\right],$$
$$m_3 = \frac{1}{4\beta(1-\rho_0)^2} - d, \qquad m_4 = \frac{\alpha}{2\beta\rho_0}, \tag{30}$$

where ρ_0 is given in the bottom line of (26).

The dependence on the chemical potential drops out in the $U(N)$ model both from the free energy and from invariant observables. Screening masses do not depend on μ.

III. N-POINT FUNCTION

In this section we briefly consider the N-point function. In the pure gauge theory ($\alpha = 0$) in the confinement phase such function is related to the potential between N static quarks (baryon potential). In order to compute the N-point function one should specify sources $\eta(x)$ and $\bar{\eta}(x)$ in Eq. (2). Let $x(i), i = 1, \ldots, N$ be positions of N static quarks on a d-dimensional lattice. Then, one takes the following values: $\eta(x(i)) = 1$, $\eta(x) = 0$ if $x \neq x(i)$ and $\bar{\eta}(x) = 0$ for all x. In the confinement region the saddle-point solutions equal that of the $U(N)$ model, Eq. (26). Expanding around these solutions, one finds after a long but straightforward algebra

$$\Gamma_N(\sigma) \sim \sum_x \prod_{i=1}^{N} G_{x,x(i)}(\sigma), \qquad \sigma = \sqrt{\frac{2}{\beta}(1 - d\beta)}, \tag{31}$$

where the sum over x runs over all lattice sites and an irrelevant constant factor is omitted. In the continuum limit the Green's function (12) takes the form

$$G_{x,x'} = \frac{\text{const}}{R^{\frac{d}{2}-1}} K_{\frac{d}{2}-1}(\sigma R), \qquad R^2 = \sum_{n=1}^{d} (x_n - x'_n)^2, \tag{32}$$

where $K_n(x)$ is the modified Bessel function of the second kind. The summation over x can now be replaced by the integration. The evaluation of $\Gamma_N(\sigma)$ reduces to the well-known geometric median problem: find a point y which minimizes the expression

$$\sum_{i=1}^{N} \sqrt{\sum_{n=1}^{d} (y_n - x_n(i))^2}\,. \tag{33}$$

It follows that the N-quark potential takes the form of the geometric median law

$$V_N(\sigma) = -\ln \Gamma_N(\sigma) \sim \sigma \sum_{i=1}^{N} |y - x(i)|. \tag{34}$$

If $N = 3$ this gives a Y law for the three-quark potential $V_3(\sigma) \sim \sigma Y$. This result agrees with Ref. [26], where it was shown via Monte Carlo simulations that the Y law dominates the three-quark potential in the $SU(3)$ Polyakov loop model. σ is a string tension of the N-quark system. It equals the quark–antiquark string tension. This elucidates how an analog of the Y law appears in the large N limit.

In the full theory with $\alpha \neq 0$ we use again the general result, Eqs. (13)–(15), to find for the N-point function above the phase transition

$$\Gamma_N \sim e^{-\mu N} M^N \exp\left[\frac{1}{4N^2\beta\rho_0^2} \frac{C_1}{\sqrt{C_1 C_2}} \sum_{i \neq j} (G_{x(i),x'(j)}(m_-) - G_{x(i),x'(j)}(m_+))\right]. \tag{35}$$

This result leads to conclusions similar to those described in Sec. II B. The most important one is that the connected part of the N-point function exhibits the oscillating behavior in the same region of parameters as the two-point functions.

IV. SUMMARY

This paper continues the investigation of Polyakov loop models at nonzero chemical potential in the 't Hooft-Veneziano limit. In [14] we have studied the general phase structure of various such models. The present paper deals with the correlation functions of the Polyakov loops and the corresponding screening masses. Our main findings are the following:

(i) Explicit formulas for the correlation functions and screening masses of $U(N)$ and $SU(N)$ Polyakov loop models with nonzero chemical potential have been obtained in the 't Hooft-Veneziano limit both in the confinement and deconfinement phases.
(ii) In the deconfinement phase we established the existence of the complex masses and an oscillating decay of correlations in a certain region of parameters.
(iii) The computation of the screening masses in different regions demonstrates that at small α the ratio $m_i/m_r \gg 1$ reaches its maximum close to the critical surface. In this region, one observes profound oscillations of correlation functions with distance.
(iv) It was shown that the calculation of the N-point correlation function reduces to the geometric median problem in the confinement phase.

In a nutshell, the paper provides a deeper understanding of the properties of the Polyakov loop models at finite density in the large N limit. Formulas (19)–(23) were used in the $SU(3)$ Polyakov loop model considered in [19]. It was found that these expressions are well suitable as a fitting ansatz for analysis of MC data for $N = 3$. It would be important and interesting to extend the results of the present paper to models with an exact static determinant and to $SU(N)$ models at other finite values of N. Such work is in progress.

ACKNOWLEDGMENTS

V. C. acknowledges support by the Deutsche Forschungsgemeinschaft (DFG, German Research Foundation) through the CRC-TR 211 "Strong-interaction

matter under extreme conditions," Project No. 315477589-TRR 211. The work of S. V. is supported by the National Academy of Sciences of Ukraine, Grant No. 0122U200259.

APPENDIX

The functions b_1, b_2, b_3 are given by

$$b_1 = \frac{2it}{s\Delta}\left[4t^4(H_2+H_4) + 4H_4 s^2t^2 + itsu(s+it)^2 + (s^2+t^2)^2\left(H_3 + u^2\ln\frac{1+u}{u}\right)\right] + \frac{2it^3}{su}, \tag{A1}$$

$$b_2 = \frac{iu^2}{2\Delta}[4stH_2 - iu(s+it)^2] + \frac{1}{2}\alpha\rho\cosh\omega, \tag{A2}$$

$$b_3 = \frac{2i\,ut}{\Delta}[4t^2H_2 + 2(s^2+t^2)H_4 - u(s+it)^2] - \alpha\sin i\omega, \tag{A3}$$

$$\Delta = 4ist(H_2H_3 - H_4^2) + u[(s+it)^2H_3 + 4istH_4 - 4t^2(H_2+H_4)] + u^2(4istH_2 + u(s+it)^2)\ln\frac{1+u}{u}. \tag{A4}$$

The functions H_2, H_3, H_4 are defined as derivatives of the function H_1

$$H_1 = \sum_{k=0}^{\infty} r^{2k+2}C_k(u), \qquad H_2 = r^2\frac{\partial^2 H_1}{\partial r^2}, \qquad H_3 = u^2\frac{\partial^2 H_1}{\partial u^2}, \qquad H_4 = ru\frac{\partial H_1}{\partial u\partial r}, \tag{A5}$$

$$C_k(u) = \sum_{m=1}^{\infty}\frac{(-4)^k(-u)^m\Gamma(k+\frac{m}{2}+1)\Gamma(2k+m)}{(k+1)(k+1)!(2k+1)!\Gamma(\frac{m}{2}+1)\Gamma(m)}, \qquad r = \sqrt{s^2+t^2}. \tag{A6}$$

The saddle-point solutions near the critical surface $z \sim 0$ read [14]

$$u_0 = y, \qquad t_0 = \frac{y}{2\rho_1}, \qquad s_0 = -i\left(\frac{\alpha}{2} + \beta d\rho_1 + \beta d\rho_2 y\right), \qquad \omega_0 = -i\frac{y}{\alpha\rho_1},$$
$$\rho_0 = \rho_1 + \rho_2 y, \qquad \rho_1 = \frac{\alpha}{2(1-\beta d)}, \qquad \rho_2 = \frac{1}{\alpha}\sqrt{1-4\rho_1^2}, \qquad y = -\frac{z}{W_{-1}(-e^{-c}z)}, \tag{A7}$$

where $W_{-1}(x)$ is a lower branch of the Lambert function and c—unessential constant.

[1] O. Philipsen, Proc. Sci., LATTICE2019 (**2019**) 273.
[2] E. Seiler, EPJ Web Conf. **175**, 01019 (2018).
[3] C. Gattringer, Nucl. Phys. **B850**, 242 (2011).
[4] Y. D. Mercado and C. Gattringer, Nucl. Phys. **B862**, 737 (2012).
[5] M. Fromm, J. Langelage, S. Lottini, and O. Philipsen, J. High Energy Phys. 01 (2012) 042.
[6] O. Borisenko, V. Chelnokov, and S. Voloshyn, EPJ Web Conf. **175**, 11021 (2018).
[7] O. Borisenko, V. Chelnokov, and S. Voloshyn, Phys. Rev. D **102**, 014502 (2020).
[8] D. J. Gross and E. Witten, Phys. Rev. D **21**, 446 (1980).
[9] S. R. Wadia, Phys. Lett. **93B**, 403 (1980).
[10] P. H. Damgaard and A. Patkós, Phys. Lett. **172B**, 369 (1986).
[11] C. H. Christensen, Phys. Lett. B **714**, 306 (2012).
[12] O. Borisenko, V. Chelnokov, and S. Voloshyn, Nucl. Phys. **B960**, 115177 (2020).
[13] O. Borisenko, V. Chelnokov, and S. Voloshyn, Proc. Sci. LATTICE2021 (**2021**) 453.
[14] O. Borisenko, V. Chelnokov, and S. Voloshyn, Phys. Rev. D **105**, 014501 (2022).
[15] A. Bazavov and J. H. Weber, Prog. Part. Nucl. Phys. **116**, 103823 (2021).

[16] J. Takahashi, K. Nagata, T. Saito, A. Nakamura, T. Sasaki, H. Kouno, and M. Yahiro, Phys. Rev. D **88**, 114504 (2013).
[17] M. Andreoli, C. Bonati, M. D'Elia, M. Mesiti, F. Negro, A. Rucci, and F. Sanfilippo, Phys. Rev. D **97**, 054515 (2018).
[18] O. Borisenko, V. Chelnokov, E. Mendicelli, and A. Papa, Nucl. Phys. **B965**, 115332 (2021).
[19] O. Borisenko, V. Chelnokov, E. Mendicelli, and A. Papa, Nucl. Phys. **B998**, 116424 (2024).
[20] P. N. Meisinger, M. C. Ogilvie, and T. D. Wiser, Int. J. Theor. Phys. **50**, 1042 (2011).
[21] H. Nishimura, M. Ogilvie, and K. Pangeni, Phys. Rev. D **93**, 094501 (2016).
[22] O. Akerlund, P. de Forcrand, and T. Rindlisbacher, J. High Energy Phys. 10 (2016) 055.
[23] O. Borisenko, V. Chelnokov, S. Voloshyn, and P. Yefanov, Phys. Lett. B **827**, 137000 (2022).
[24] G. 't Hooft, Nucl. Phys. **B72**, 461 (1974).
[25] G. Veneziano, Nucl. Phys. **B117**, 519 (1976).
[26] O. Borisenko, V. Chelnokov, E. Mendicelli, and A. Papa, Nucl. Phys. **B940**, 214 (2019).